An Optimized Medium-Transparent MAC Protocol for Multi-service FiWi 5G transport networks

G. Kalfas[*,†], M. Gatzianas[*,†], D. Palianopoulos[*,†], A. Mesodiakaki[*,†], C. Vagionas[*,†], R. Maximidis[*,†], A. Miliou[*,†] and N. Pleros[*,†]

[*]Department of Informatics, Aristotle University of Thessaloniki, Thessaloniki, Greece

[†]Center for Interdisciplinary Research and Innovation, Thessaloniki, Greece

Emails: {gkalfas, mgkatzia, dpaliano, amesodia, chvagion, maximidis, amiliou, npleros}[at]csd.auth.gr

***Abstract*— We present an optimized Medium-Transparent MAC (oMT-MAC) protocol for Analog-RoF Fiber-Wireless 5G and beyond X-haul networks, capable of generating an optimum transmission schedule, which boosts the protocol's efficiency by utilizing the full delay budget of higher priority flows. Results show that oMT-MAC's optimization model can reduce delays by up to 20% for low-priority flows while maintaining the 5G Fronthaul and URLLC KPIs.**

Keywords*— *Analog Radio-over-Fiber; 5G; Fronthaul; Fiber-Wireless; Medium Transparent MAC (MT-MAC); Optimization;

I. INTRODUCTION

5G New Radio (NR)'s adoption of mmWave radio has been a key driver in achieving the enormous 5G peak and user data rates KPIs set by ITU and 3GPP. However, higher frequencies require intensive Radio Access Network (RAN) densification, which in turn places a burden on the Mobile Network Operators' (MNO's) infrastructure to transport the massive amounts of data from the remote locations back to the 5G core. To offer the required RAN flexibility without costly fiber-trenching, the industry has been actively working on combined Fiber-Wireless (FiWi) RAN transport [1], as a viable solution for Front-, Mid-, and Back-haul (X-haul) applications.

As FiWi solutions are deployed however, the efficiency of Layer-2 protocols for converged networks has come into the spotlight. Radio and Fiber (R&F) and Radio-over-Fiber (RoF) are two classifications frequently used to categorize FiWi networks. In R&F networks, protocol translation occurs at the interface of each discrete network segment, which implements its own MAC layer scheduler. However, R&F networks can only be used in decentralized RANs (D-RANs), which are less efficient for usage in densely populated cities [2]. To this purpose, Analog-RoF (A-RoF) has received significant attention for convergent FiWi networks because of its advantages in terms of spectrum efficiency and the minimal complexity of the analog Remote Antenna Units (RAUs) [3]. As wireless signals traverse both the optical and wireless domains, the latter must be jointly administered for A-RoF FiWi networks to offer the best end-to-end(E2E) performance. To this end, new medium-transparent protocols must be developed for optimally allocating the converged wireless and optical resources. For FiWi networks with A-RoF, a Medium Transparent-Medium Access Control (MT-MAC) protocol was initially introduced in [4]. Between the MT-MAC Central Office (CO) and the wireless nodes, this protocol dynamically controls both optical and wireless resources. Hence, the CO directly administers the amount of optical and wireless resources for RAUs and nodes, respectively. In MT-MAC, data exchange takes place by sending polling packets to each node authorized for transmission in accordance with a Polling Sequence (PS). These packets are divided into Superframes (SFs), whose size depends on the specific MT-MAC protocol. A static SF size was used in the first iteration of the MT-MAC protocol [4], independently of the load or number of served nodes. In [5], a modification of [4] that reduces handover latency by using predictions of the remaining wireless capacity was proposed. In [6], a method for reducing the number of polling packets required to count all active users was described, and in [7], traffic classes were introduced to MT-MAC for support of Quality-of-Service (QoS). The first MT-MAC version with non-static SF sizes was given in [8], where the CO allots transmission windows to each RAU proportionately to the number of its active users, albeit without considering the real load on each node. The latter was achieved by Gated-MT-MAC (gMT-MAC) [9], which used the Gated service paradigm for establishing the SF duration to significantly outperform [4], [8] by up to 20X higher throughput and 2X lower delay. However, gMT-MAC lacks the QoS features to effectively handle traffic with variable bandwidth, latency/jitter criteria, as envisioned by 5G-NR's RAN disaggregation into Centralized/ Distributed/Remote units (CU/DU/RUs).

Recent State-of-the-Art (SoA) QoS-aware MT-MAC (qMT-MAC) protocols [10] were created to provide QoS assurances under concurrent X-haul traffic flows and were shown to fulfill the corresponding latency and jitter 3GPP criteria. However, the PS created in qMT-MAC schedules the different traffic classes in a specific order, i.e., higher priority packets are always placed first in the PS, followed by medium priority packets, and best effort packets are scheduled last in any remaining slots. As express packets are scheduled in earlier slots, their latency is decreased at the expense of lower-priority traffic. Nevertheless, the latency KPIs for 5G flows typically have a "threshold" property, where any packets with an achieved latency less than a certain limit are considered to meet their QoS requirements and no QoS improvement is achieved if the experienced packet latency is further reduced. Fronthaul traffic, such as splits 7.2 and 6 with latency requirements of 100μs and 250μs, respectively, are typical examples of threshold-based KPIs, as is Ultra-Reliable Low Latency Communications (URLLC) traffic with a latency budget of 1ms [11]-[14]. This observation suggests that it may be possible to schedule lower-priority packets before express packets, as long as the latter meet their latency KPIs, clearly improving the lower-priority flow performance.

However, applying this approach to concurrent flows of multiple express traffic classes, with different latency KPI requirements, is not straightforward without an underlying model. Exploiting the above threshold QoS properties of express services, this paper proposes and evaluates an optimized MT-

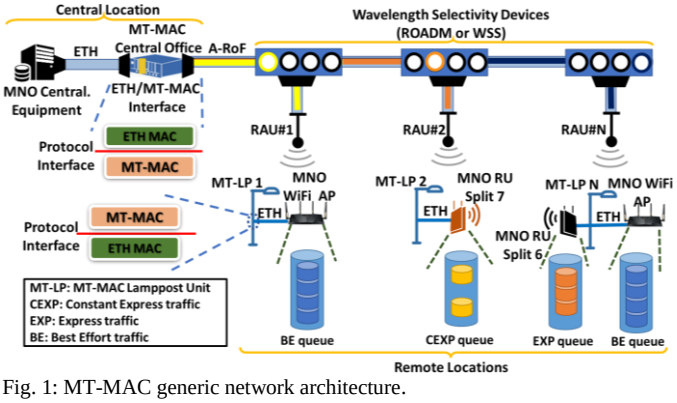

Fig. 1: MT-MAC generic network architecture.

MAC (oMT-MAC) protocol that employs a Mixed Integer Linear Problem (MILP) model formulation to construct an optimal PS capable of delaying higher-priority packets intelligently and dynamically, without violating their respective KPIs, at the benefit of faster lower-priority traffic service. Thus, oMT-MAC transforms the usual zero-sum game relationship between express and best-effort traffic into a positive-sum game, increasing protocol efficiency without sacrificing 5G service requirements. Although optimization models have been employed in scheduling, both as MILP formulations (e.g., joint functional split selection and scheduling in C-RANs [15], optimal resource allocation in disaggregated RANs [16]) and as conflict-graph formulations (e.g., scheduling of time-triggered flows [17]), they are not directly applicable to MT-MAC protocols, having either different scope or underlying assumptions. Our proposed model is specially tailored for MT-MAC protocols and, to the best of our knowledge, represents the 1st attempt towards optimization-driven quantitative guarantees.

The rest of the paper is organized as follows: In Section II, the system model is presented. In Section III, the oMT-MAC protocol and its novelties are described. Section IV presents the oMT-MAC's performance evaluation, while Section V concludes the paper. Calligraphic letters (e.g., $\mathcal{A}$) denote sets, $\setminus$ denotes set difference and $\mathbb{I}[X]$ denotes the indicator of a Boolean X (i.e., $\mathbb{I}[X] = 1$ if X is true, 0 otherwise).

II. System Model

We assume a 5G FiWi PtMP transport network with a central site connected to multiple remote sites, as shown in Fig. 1. The centralized MNO hardware is installed at the central site, which can include a 5G core baseband unit (CU) or CU+DU. The MT-MAC CO is connected to the central MNO devices via Ethernet and the protocol is translated on their interface, i.e., CO extracts the Ethernet payload, encapsulates it into MT-MAC packets and modulates them onto A-RoF carriers that reach, through the RAUs, the MT-MAC Lamppost Units (MT-LPs). The MT-LPs establish Ethernet connection with the remote MNO equipment. The remote MNO equipment can either be a 5G Base Station, a DU+RU module, or an RU module. At the CO-to-RAU segment, a set of wavelength pairs is used, one of which is used for Uplink (UL) communication and the other for Downlink (DL) communication. Higher resource utilization is attained at the network's fiber segment by using Wavelength Division Multiplexing (WDM), which enables the delivery of several wavelengths over the same fiber. A common Control Channel (CC), is also employed for network management purposes.

We consider UL traffic generated by MNO nodes in the remote sites and directed to the MNO centralized equipment. At each RAU, a Wavelength Selectivity Device (WSD), such as a Reconfigurable Optical Add-Drop Multiplexer (ROADM) or a Wavelength Selective Switch (WSS), is used for wavelength allocation (Fig. 1). For communication between the MNO nodes and MT-LPs, the Ethernet-based enhanced Common Public Radio Interface (eCPRI) X-haul protocol is used. We consider the following 3 traffic classes, reflecting specific eCPRI splits:

- Constant Express traffic (CEXP), which has strict criteria for delay and jitter, simulates low-split Constant Bit Rate (CBR) fronthaul communication. 3GPP splits 7 and 8 are two examples of this form of traffic [11]. According to eCPRI, CEXP traffic must have one-way delay up to 100 μs and jitter up to 65 ns [12].
- Express traffic (EXP) simulates fronthaul traffic with a load-dependent traffic pattern [12] similar to 3GPP split 6. We assume that EXP traffic delay should not exceed 250 μs [13].
- Best Effort (BE) traffic: With lax restrictions, this load-varying traffic simulates all other X-haul traffic types, such as midhaul/backhaul traffic and 3GPP splits higher than 6.

Each MT-LP serves as a traffic aggregator for the MNO equipment, as for instance depicted at MT-LP N, visible in the lower-right corner of Fig. 1. We consider a time-slotted system, with slot indices $t = 1,2, \ldots$, designed to support the above 3 traffic types, and assume that packets of these flows arrive randomly at the beginning of a slot. Let $\mathcal{C}$ be the set of supported traffic flows, where traffic flow $c \in \mathcal{C}$ is denoted as $c = (T_c, \langle d_c \rangle)$, with T_c a flow type/class identifier taking one of the values *"CEXP"*, *"EXP"*, *"BE"*, and $\langle d_c \rangle$ an (optional) tuple whose semantics depend on T_c. Specifically, for $T_c =$ *"CEXP"*, we define $\langle d_c \rangle \triangleq \langle uid_c, IFG_c \rangle$, where uid_c is a unique CEXP flow id and IFG_c is an integer indicating the time interval, in slots, between two consecutive arrivals of packets belonging to the CEXP flow. To this end, the IFG_c value determines the load induced by CEXP flow c. Hence, CEXP traffic flow $c = (\textit{"CEXP"}, \langle uid_c, IFG_c \rangle)$ has its packets ***a priori*** scheduled in slots belonging to the set $\mathcal{S}_c \triangleq \{is_c + k \cdot IFG_c : k \in \mathbb{N}\}$, where $is_c > 0$ is the slot of the first (i.e., earliest) scheduled packet for this flow. We also assume that the is_c values are properly selected to avoid conflicts among different CEXP flows. For $T_c =$ *"EXP"*, we define $\langle d_c \rangle \triangleq \langle \tau_c \rangle$, with τ_c the maximum tolerated queueing delay, i.e., the time difference (in slots) between the slot where the packet is (eventually) scheduled for transmission and the packet's arrival slot. The E2E latency KPI can be easily converted into an equivalent maximum queueing delay τ_c by accounting for the transmission/propagation delay, which is assumed to be constant for all packets of ***a flow along a given path***. Finally, since there is a ***single BE traffic flow***, for $T_c =$ *"BE"*, $\langle d_c \rangle$ is empty. Each packet u is characterized by the tuple $\langle c_u, i_u \rangle$ where c_u is the packet's flow as defined above, and i_u is the packet's index, where we assume that each packet is ***globally and uniquely*** identified by the pair (c_u, i_u), so that we hereafter drop the u subscript and refer to "packet (c, i)".

III. The oMT-MAC Protocol

This Section outlines the functionality of oMT-MAC, which has some features in common with other SoA MT-MAC protocols (i.e., qMT-MAC [10]), as briefly discussed in Section III-A. Section III-B focuses on oMT-MAC's novel properties. We direct the reader to [10] for a detailed recap of qMT-MAC.

A. Features common to all MT-MAC protocols

The CO manages all UL data plane packet scheduling. There are two distinct Contention Periods (CPs); the 2nd CP seeks to determine the Buffer Status (BuS) of each active MT-LP in order to allocate the proper Transmission Windows, and the 1st CP identifies which RAUs are connected to MT-LPs serving active MNO nodes. In the 1st CP, the CO designates wavelengths for data communication at the "active" RAUs and cycles through the RAUs in Round Robin (RR) fashion if the number of RAUs containing active MT-LPs exceeds the number of available wavelengths (see Fig. 2 in [10]).

In the 2nd CP, the CO exchanges Resource Request Frames to obtain BuS data, including the MAC address of each MT-LP with unprocessed packets in its buffer, as well as the quantity and traffic class of these packets (see Fig. 3(a) in [10]). The 2nd CP ends when all active MT-LPs have successfully transmitted their RRFs, and the DATA_TX period, comprising a series of Data Frames (DFs), starts. Sending and receiving DATA_POLL, DATA, and ACK packets are parts of every DF. The CO broadcasts DATA_POLL packets that specify the type of packet (i.e., CEXP, EXP, or BE) and the maximum number of packets of that type the MT-MAC client can transmit after receiving the DATA_POLL. The DATA_POLL payload is generated according to the PS, described in Section III-B for oMT-MAC, and depends on the specific MT-MAC protocol. The CO then sends an ACK packet to the MT-LP to confirm successful data reception after the MT-LP node transmits the appropriate data packets in response to the DATA POLL reception. A SuperFrame (SF) contains all DFs inside a single PS. For efficiency, MT-LPs can piggyback their data onto the most recent DF transmission of the active SF.

B. Optimization-driven PS creation in oMT-MAC protocol

Define ***cycle*** $l = 1,2,\ldots$, as the time interval of N_{cy} consecutive slots in set $\mathcal{R}_l \triangleq \{(l-1)\cdot N_{cy}+1, \cdots, l\cdot N_{cy}\}$. oMT-MAC performs scheduling on a cycle basis as follows:

• within cycle l, the transmission of CEXP packets is a priori scheduled for the slots in set $\mathcal{S}^l_{CEXP} \triangleq \mathcal{R}_l \cap \left(\cup_{c:T_c="CEXP"} \mathcal{S}_c\right)$. Hence, only the remaining slots in set $\mathcal{A}^l \triangleq \mathcal{R}_l \setminus \mathcal{S}^l_{CEXP}$ are available for serving EXP or BE traffic during cycle l.

• at the start of cycle l, oMT-MAC schedules EXP/BE packets in the slots of $\mathcal{A}^l$ by solving an optimization problem to be formulated below. It is possible that some of the packets queued at the start of cycle l are not scheduled in cycle l. Also, any EXP/BE packets arriving after the first slot of $\mathcal{R}_l$ in cycle l are not considered for scheduling during cycle l but become available for scheduling in the cycle $(l+1)$.

Let $a^l_{c,i}$ be ***the number of slots*** that packet (c,i) has been stored in queue Q_c until the start of cycle l. Let A^l be the cardinality of $\mathcal{A}^l$ and denote with N^l_c the number of packets stored in Q_c at the start of cycle l. The maximum number of packets that can be scheduled in cycle l is $N^l_{max} \triangleq min\left(A^l, N^l_{BE} + \sum_{c:T_c="EXP"} N^l_c\right)$. Let $x^{c,l}_{i,j} \in \{0,1\}$ be the Boolean indicator of whether EXP/BE packet (c,i) is scheduled at slot j in cycle l. If packet (c,i) is indeed scheduled in cycle l, the total number of slots it has been enqueued until its transmission is $T^l_{c,i} = a^l_{c,i} + \sum_{j\in\mathcal{A}^l}\left(j - l\cdot N_{cy}\right)x^{c,l}_{i,j}$; otherwise at the start of the next cycle, it will hold $a^{l+1}_{c,i} = a^l_{c,i} + N_{cy}$.

For EXP flow packets, we introduce decision variables $v^l_{c,i} \triangleq \mathbb{I}[T^l_{c,i} > \tau_c]$ to determine whether the queuing delay of EXP packet (c,i) has violated the delay requirement τ_c in cycle l, and transform the above definition into:

$$\begin{aligned} &v^l_{c,i} \in \{0,1\}, \ \ \forall (c,i): T_c = \ "EXP", \\ &v^l_{c,i} \geq \frac{a^l_{c,i} + \sum_{j\in\mathcal{A}^l}(j - l\cdot N_{cy})x^{c,l}_{i,j} - \tau_c}{M}, \ \ \forall (c,i): T_c = \ "EXP", \end{aligned} \tag{1}$$

where $M \triangleq \max_{c,i:\, T_c="EXP"}\left(a^l_{c,i} + N_{cy}\right)$ is selected so that the right-hand side of the second expression in (1) is ***strictly*** less than 1. We introduce a penalty $p_c > 0$ ***for each*** EXP packet (c,i) whose queueing delay exceeds τ_c (i.e., if it holds $v^l_{c,i} = 1$), and define the total EXP-based penalty P^l_{EXP} in cycle l as:

$$P^l_{EXP} \triangleq \sum_{(c,i):T_c=\ "EXP"} p_c v^l_{c,i}\,, \tag{2}$$

and seek to minimize P^l_{EXP} for each cycle l. The separability of $v^l_{c,i}$ in (2), combined with the fact that $p_c > 0$ for all c, implies that minimizing P^l_{EXP} with respect to $v^l_{c,i}$ automatically satisfies the condition $v^l_{c,i} = \mathbb{I}[T^l_{c,i} > \tau_c]$.

Although no delay requirements are associated with BE flows, achieving low delay for scheduled BE packets while still minimizing P^l_{EXP} is obviously beneficial performance-wise. Hence, we employ a multi-objective formulation and introduce a secondary objective based on the average BE packet delay. To this end, we compute in (3) the accrued queueing delay for packet (BE,i) at the end of cycle l, viz.:

$$\begin{aligned} T^l_{BE,i} \triangleq a^l_{BE,i} + \sum_{j\in\mathcal{A}^l}\left(j - l\cdot N_{cy}\right)x^{BE,l}_{i,j} + \\ + N_{cy}\left(1 - \sum_{j\in\mathcal{A}^l} x^{BE,l}_{i,j}\right), \end{aligned} \tag{3}$$

where the second and third terms in (3) capture, respectively, whether packet (BE,i) is scheduled (or not) within cycle l. We also impose the following natural constraints:

$$\sum_{(c,i):T_c\in\{"EXP","BE"\}} \sum_{j\in\mathcal{A}^l} x^{c,l}_{i,j} = N^l_{max}, \tag{4}$$

$$\sum_{j\in\mathcal{A}^l} x^{c,l}_{i,j} \leq 1\,, \qquad \forall (c,i): T_c \in \{"EXP","BE"\}, \tag{5}$$

$$\sum_{(c,i):T_c\in\{"EXP","BE"\}} x^{c,l}_{i,j} \leq 1, \qquad \forall j \in \mathcal{A}^l, \tag{6}$$

where, for each cycle l, (4) imposes the condition that no available slots are left un-utilized, (5) guarantees that each packet can be scheduled in at most one slot within the cycle, and (6) prohibits multiple packets from being scheduled into the same slot. Hence, the creation of the PS has been reduced to the following multi-objective MILP formulation:

$$\begin{aligned} &Lex\_min\left(P^l_{EXP}, \sum_i T^l_{BE,i}\right), \\ &\text{s.t} \quad (1)\text{-}(6), \ x^{c,l}_{i,j} \in \{0,1\}, \end{aligned} \tag{7}$$

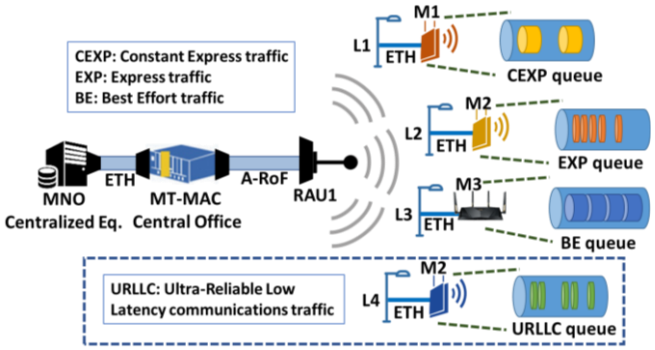

Fig. 2: Network configuration in simulation for performance evaluation

with unknown variables $x_{i,j}^{c,l}$, $v_{c,i}^{l}$ where Lex_min is lexicographic minimization. oMT-MAC solves (7) for each cycle l and iteratively updates the values $a_{c,i}^{l}$ of all non-scheduled EXP/BE packets at the end of cycle l.

IV. Performance Evaluation

To assess the performance improvements of oMT-MAC over SoA qMT-MAC, we present an extensive performance evaluation based on the OMNET++ simulator and CPLEX MILP solver suites. In all subsequent results, the SF duration is set equal to the cycle length of N_{cy} slots. Although efficient greedy heuristic algorithms with polynomial time complexity can be proposed for (7), the analysis and evaluation of such heuristics is outside the paper's scope, which does not diminish the value of the CPLEX solution as a benchmark tool.

A. Single load-dependent EXP traffic flow scenario

We employ the setup depicted in Fig. 2, where a single RAU is wirelessly connected to MT-LPs L1, L2 and L3, with each one connected to a CEXP, EXP and BE traffic generator respectively (*L4 is not present in this setup*). Fig. 3 presents the average packet delay (in ms) vs. normalized load for both oMT- and qMT-MAC protocols, for both EXP and BE traffic flows, and for three IFG values, i.e., 5, 10 and 20, that characterize the CEXP traffic. Note that IFG=5 implies that CEXP traffic induces 20% (1/5th) of the normalized network load, as well as that the SF duration is set to 5 slots, with the first out of every 5 slots being reserved for a CEXP packet. Fig. 3(a) and 3(b) present the results for the EXP and BE traffic flows, respectively. Normalized load corresponds to the produced traffic as a percentage of the channel bitrate, i.e., a normalized load of 0.1 corresponds to generated traffic rate equal to 10% of the channel bitrate. Additionally, the load value refers individually to the EXP and BE flows, i.e., 0.1 load denotes that the EXP and BE flows individually produce packet traffic equal to 10% of the channel bitrate each, thus yielding a 20% aggregate load for both traffic types. By means of Fig.3(a), it can be seen that for all IFG values, oMT-MAC provides worse results for average EXP delay than its qMT-MAC counterpart, when load is greater than 10% per flow (20% EXP and BE aggregated). This is the expected behavior since oMT-MAC essentially chooses to delay the EXP packets in favor of the BE packets, provided that the EXP packets are not scheduled beyond their designated maximum delay value τ_c (250μs in this specific evaluation). As observed, the EXP packet delay performance gap between the oMT- and qMT-MAC protocols becomes greater as load increases; however, the oMT-MAC's delay performance

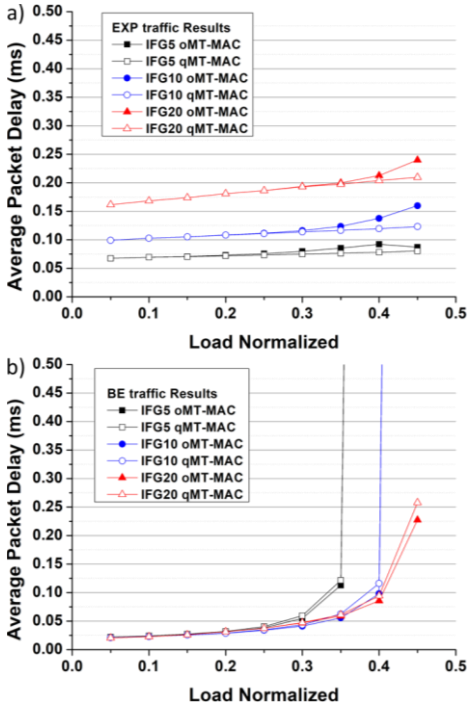

Fig. 3: oMT- vs. qMT-MAC results for IFG values 5,10,20. Lines with filled, (resp. hollow) symbols refer to oMT-MAC (resp. qMT-MAC). a) EXP traffic results, b) BE traffic results.

remains always below 250μs, attesting to the fact that the optimization model prioritizes the EXP delay violation criterion. The increased performance gap that comes with increased load values appears because, in larger loads, more BE packets are awaiting transmission, and therefore oMT-MAC's optimization model delays the EXP packets at a greater extent, leading to larger overall EXP packet delays. One notable behavior is that in the case of IFG=5 (i.e., 5 slots per SF, 4 of them available for EXP and BE traffic) at 45% normalized load per flow, oMT-MAC's delay drops instead of increasing. This is due to the fact that the network is already oversaturated (i.e., 20% load from CEXP, 45% each from EXP and BE, totaling 110%) and since only 4 slots are available per SF cycle, oMT-MAC does not have enough slots to stall outstanding EXP packets. In the cases of IFG=10 and 20 however, with more slots available per SF, when load is increased at 45% per flow, oMT-MAC still has the ability to delay the EXP packets in favor of the BE packets. The opposite behavior is evident in Fig. 3(b), where it is observed that BE packets perform better under oMT-MAC, achieving lower delay under most tested load conditions. The BE delay performance gap between oMT-MAC and qMT-MAC increases along with the IFG increment, due to the greater SF duration, which enables oMT-MAC to place EXP packets in later slots within the SF, while at the same time freeing earlier slots that can be used by BE packets. BE traffic results for both qMT-MAC and oMT-MAC also show that increased IFG values push the BE traffic saturation values to higher loads, i.e., the higher the IFG values, the higher load can be sustained by the BE traffic until BE delay increases rapidly. This is because higher IFG values imply lower CEXP loads, thus decreasing the background network traffic, allowing for more BE packets to be served.

Fig. 4 presents the performance of oMT-MAC against qMT-MAC as the relative percentage difference between the qMT- and oMT-MAC values (i.e., positive/negative values mean that

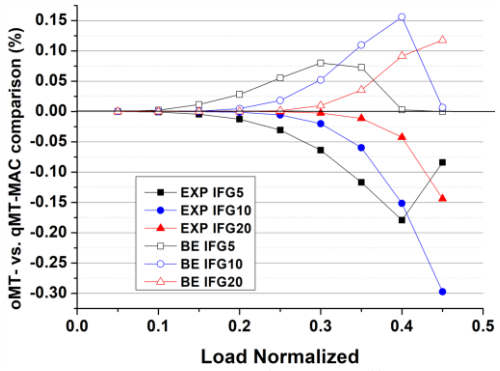

Fig. 4: oMT- vs. qMT-MAC delay performance difference as percentage.

oMT-MAC delays are lower/higher, respectively, than qMT-MAC). For instance, a value of 0.1 means that the oMT-MAC delay is 10% lower than the respective qMT-MAC values, whereas a value of -0.1 means that the oMT-MAC delay is 10% higher. By means of Fig. 4, greater gains for the BE traffic delay, and respectively greater losses for the EXP traffic, can be observed at IFG=10 and 20 compared to IFG=5, due to the combined effect of lower background CEXP traffic load and a higher number of available scheduling slots in the SF that allow for more flexibility by the oMT-MAC model. In Fig. 4 one can notice that minimal gains and losses are observed at low loads for all IFG values. This is due to the fact that, at low loads, there are only a few arriving BE and EXP packets that are being served very fast, as queues are mostly empty and, therefore, no large gains can be produced. At medium loads, the gains/losses become higher, as oMT-MAC can fit all traffic to the available slots, while also maintaining the flexibility to delay EXP packets in favor of BE packets, provided that EXP packet delay remains less than the target of 250μs. At high loads, we observe again diminishing gains for the BE traffic due to the fact that, at high loads, the increased number of arriving/enqueued EXP packets translates to higher delays, therefore forcing oMT-MAC to schedule them ahead of BE packets to avoid violating the EXP delay constraints and, accordingly, minimize P_{EXP}^{l} defined in (2) (note that this is the primary objective and takes precedence over the BE delay minimization). Overall, BE traffic delay under oMT-MAC is decreased significantly and up to 15%, compared to qMT-MAC, without the EXP packets violating their predefined delay constraint. Finally, it is worth pointing out that the maximum gain w.r.t. BE packet delay is met at IFG=10. This is due to the fact that the large SF size at IFG=20 causes the protocol's performance deterioration since the PS is constructed at the beginning of each cycle/SF, and as such, EXP packets that are generated while the PS is computed, have to wait a large amount of slots before being transmitted. To this end, more EXP packets are accumulated at the subsequent SFs, and since the delay constraint of EXP packets is always the primary criterion of the optimization model, fewer BE packets are assigned to empty slots, resulting in lower overall BE performance.

B. Dual load-dependent EXP traffic flows scenario

Contrary to qMT-MAC, the oMT-MAC protocol can distinguish between express traffic types and can produce an optimized schedule prioritizing the strictest flows, while still allowing for short delays in favor of BE and/or more relaxed express packets. This section presents a performance evaluation for the setup presented in Fig. 2 with the addition of MT-LP L4 that produces URLLC-type of traffic featuring a latency requirement of <1 ms. The 1 ms limit, used here for simplicity, accounts for the delay in the FH segment, but since τ_c is a parameter in the system model, it can be adjusted to reflect the total delay up to Application Function server.

Fig. 5 presents the average packet delay results for both oMT- and qMT-MAC protocols for three IFG values (i.e., 5, 10 and 20). As before, the load value refers to each of the EXP, URLLC, BE flows, i.e., 0.1 load means that the EXP, URLLC and BE flows each produce packet traffic equal to 10% of the channel bitrate, for a total aggregate traffic of 30%. Fig. 5(a) shows that oMT-MAC provides, again, worse results for EXP traffic delay than its qMT-MAC counterpart for almost all IFG values. As noted in the previous scenario, the performance gap between the oMT- and qMT-MAC protocols becomes greater as IFG increases, with overall delay values increasing as IFG values grow. The latter is again attributed to the fact that the larger IFG values produce greater SF cycles, where newly arrived packets (i.e., packets arriving within the current SF) have to wait for the next cycle/SF to be scheduled and transmitted. Notably, for IFG=20 at load 0.4, oMT-MAC achieves lower EXP delay than qMT-MAC (instead of higher), maintaining its average delay target below 250 μs. This is achieved by scheduling the more delay-sensitive EXP packets in contiguous slots towards the beginning of the SF, before the less urgent URRLC packets. On the contrary, qMT-MAC is observed to produce an average delay of >300 μs at these conditions, as it cannot distinguish between EXP and URLLC types of traffic, treating them at an equal base, serving them both in a RR fashion. This performance difference highlights oMT-MAC's capability to distinguish between two (or more) different types of Express traffic concurrently served

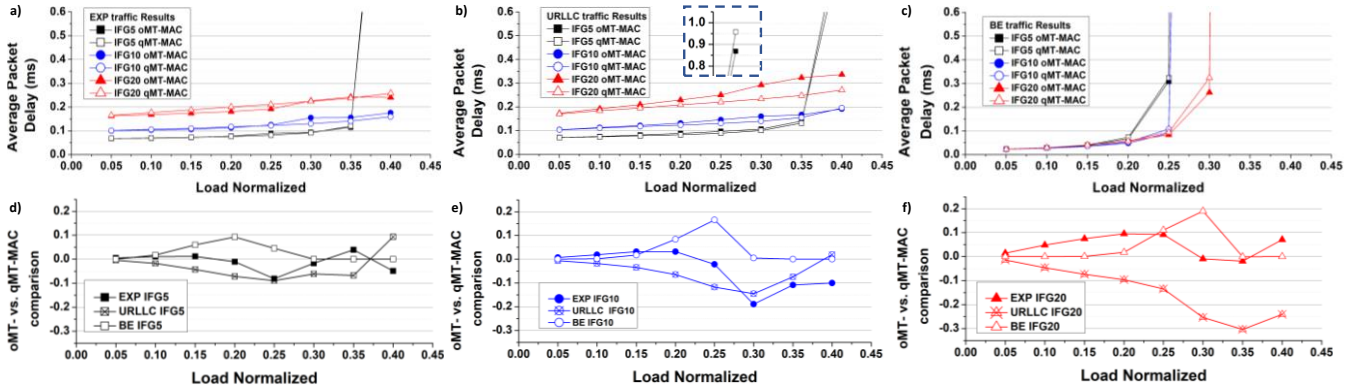

Fig. 5: oMT- vs. qMT-MAC for EXP, URLLC and BE traffic and three IFG values: a) EXP traffic results, b) URLCC traffic results, c) BE traffic results, d) performance difference for IFG=5, e) performance difference for IFG=10, f) performance difference for IFG=20.

in the same network and provide the optimal PS schedule. By means of Fig. 5(b), we can observe that URLLC traffic presents the same overall behavior as EXP traffic, i.e., oMT-MAC achieves higher URLLC delays for all IFG values compared to qMT-MAC. This is because oMT-MAC takes into account that URLLC traffic can withstand up to 1 ms delay, and therefore opts for delaying URLLC packets in favor of BE packets, as long as the 1 ms requirement is achieved, which, as attested by Fig. 5(b). The larger IFG values cause a longer SF duration, which provides more flexibility to the oMT-MAC model to induce further delays to the URLLC packets. Finally, Fig. 5(c) shows that, as in the scenario of Section IV.A, oMT-MAC offers significant performance gains to the BE traffic flows that become greater as IFG values increase, due to the greater SF duration. Besides the oMT-MAC BE performance gains, BE traffic results again show that the increased IFG values push the BE traffic saturation values to higher loads.

In order to better visualize the performance difference between the oMT- and qMT-MAC protocols, Fig. 5(d)-(f) displays the respective performance gains and losses of the oMT-MAC protocol, as a percentage against the performance of the qMT-MAC protocol. By means of Fig. 5(d) it can be seen that oMT-MAC BE traffic delay is reduced up to 10% for a medium/high normalized load equal to 20% (corresponding to an aggregated load of 80% when accounting for all four traffic flows incl. CEXP), while no gains are observed at very low (i.e. 5% load per single flow, 35% aggregated) and very high loads (>30% single flow, 110% aggregated), for the reasons explained in Section IV.A. Regarding the EXP traffic flow, it can be seen that, for normalized load up to 17.5%, oMT-MAC derives small performance gains relative to qMT-MAC, since the optimization model gives precedence to the more urgent EXP packets vs. the URLLC packets, as opposed to qMT-MAC which performs RR scheduling between the EXP and URLLC flows. At medium loads, the EXP flow incurs a slightly higher delay in oMT-MAC, due to the exploitation of the available time window in favor of the BE flow. At 35% single-flow load (i.e., 3x35=105% aggregated load of EXP/URLLC/BE flows plus 20% from CEXP flow, totaling 125%), EXP flow experiences again small gains, as the network is strongly saturated and oMT-MAC's optimization model gives higher priority to EXP flow (as opposed to qMT-MAC's RR scheduling). Finally, in the highest normalized load of 40% (i.e. 120% aggregated URLLC/EXP/BE flows plus 20% from CEXP flow, totaling 140%), oMT-MAC shows minor performance losses for EXP packets due to the fact that in these very high loads, some packets have already violated the designated delay constraint even at the start of the SF cycle, in which case oMT-MAC's optimization model chooses to disregard these packets entirely (providing the only case where a violation of EXP traffic threshold is recorded as attested by Fig. 5(a)) in favor of the URLLC packets that can still be transmitted within their time limits. Finally, regarding the URLLC traffic flow, it can be seen that, with the exception of the highest load condition as explained previously, oMT-MAC displays URLLC performance losses for almost all tested loads, as the more relaxed 1 ms one-way delay constraint for URLLC is exploited towards producing delay gains for the BE traffic flow. BE flow performance for IFG values of 10 (Fig. 5(e)) and 20 (Fig. 5(f)) clearly show that BE flows achieve performance gains as the IFG values grow, reaching up to 16% for IFG=10 and almost 20% gains at IFG=20. The BE performance gains peaks are witnessed at higher load conditions as more BE packets arrive and can take advantage of the delayed EXP and URLLC packets.

V. Conclusions

The proposed oMT-MAC protocol offers an optimized PS creation process to enhance BE traffic flows by taking advantage of the threshold nature of EXP traffic delay requirements. For a single EXP traffic flow, oMT-MAC was found to produce BE delay reductions of up to 15%, without violating the EXP traffic restrictions of 250μs. For two types of express traffic, i.e., EXP and URLLC, the BE flows managed to achieve a 20% gain, again without violations of the express traffic constraints.

Acknowledgment

This work is supported by projects 5G-COMPLETE (GA871900), OCTAPUS (GA101070009) and ETHER. ETHER has received funding from the Smart Networks and Services Joint Undertaking (SNS JU) under the EU's Horizon Europe research and innovation programme (GA101096526).

References

[1] F. Yaghoubi et al., "A techno-economic framework for 5G transport networks", IEEE Wireless Communications, vol. 25, no. 5, 2018.

[2] https://www.ericsson.com/en/blog/2021/5/exploring-new-centralized-ran-and-fronthaul-opportunities

[3] S. Jacobs S. Rommel et al., "Towards a Scaleable 5G Fronthaul: Analog Radio-over-Fiber and Space Division Multiplexing", J. Lightw. Technol., vol. 38, no. 19, Oct. 2020.

[4] G. Kalfas and N. Pleros, "An agile and medium-transparent MAC protocol for 60 GHz radio-over-fiber local access networks", J. Lightw. Technol., vol. 28, no. 16, Aug. 15, 2010.

[5] Z. Xu, et al., "Multichannel resource allocation mechanism for 60 GHz radio-over-fiber local access networks", J. Opt. Commun. Netw., vol. 5, no. 3, Mar. 2013.

[6] A. Panagiotakis et al., "Performance increase for highly-loaded RoF access networks", IEEE Com. Lett., vol. 19, no. 9, Sep. 2015.

[7] E. Datsika et al., "QoS-Aware Resource Management for Converged Fiber Wireless 5G Fronthaul Networks", Proc. IEEE Global Communications Conference (GLOBECOM), 2018.

[8] G. Kalfas et al., "Client-weighted medium-transparent MAC protocol for user-centric fairness in 60 GHz radio-over-fiber WLANs", J. Opt. Commun. Netw., vol. 6, no. 1, Jan. 2014.

[9] A. Mesodiakaki et al., "A Gated Service MAC Protocol for Sub-Ms Latency 5G Fiber-Wireless mmWave C-RANs", IEEE Trans. on Wireless Commun., vol. 20, no. 4, April 2021.

[10] G. Kalfas et.al., "A QoS-Enabled Medium-Transparent MAC Protocol for Fiber-Wireless 5G RAN Transport Networks", Appl. Sci. 2022.

[11] M. Larsen et al., "A Survey of the Functional Splits Proposed for 5G Mobile Crosshaul Networks," IEEE Com. Surv. &Tut., vol.21, no. 1.

[12] Common Public Radio Interface (CPRI) Specification V7, 2015 [Online Accessed: May 2023], Available: http://www.cpri.info/downloads/CPRI_v_7_0_2015-10-09.pdf .

[13] 3GPP Release 14, TR 38.801 V14.0.0 (2017-03)

[14] TR, 38.913, "5G; Study on Scenarios and Requirements for Next Generation Access Technologies (Release 16)", Jul. 2020.

[15] I. Koutsopoulos, "Optimal functional split selecting and scheduling policies in 5G Radio Access Networks", Proc. ICC Wrkshops, 2017.

[16] M. Klinkowski, "Optimization of latency-aware flow allocation in NGFI networks", Computer Communications, vol. 161 (1), Sep. 2020.

[17] J. Falk et al., "Dynamic QoS-aware traffic planning for Time-Triggered flows in the Real-tune Data Plane", IEEE Trans. Network and Service Management, vol. 19, no. 2, June 2022.